

# Uniaxial anisotropy and temperature driven magnetization reversal of Fe deposited on a MnAs/GaAs(001) magnetic template

Maurizio Sacchi,<sup>1,2</sup> Massimiliano Marangolo,<sup>3</sup> Carlo Spezzani,<sup>4</sup> Leticia Coelho,<sup>5</sup> Romain Breitwieser,<sup>2,3</sup> Julian Milano,<sup>6</sup> and Victor H. Etgens<sup>3</sup>

<sup>1</sup>Synchrotron SOLEIL, B.P. 48, 91192 Gif-sur-Yvette, France

<sup>2</sup>Laboratoire de Chimie Physique-Matière et Rayonnement, UPMC Paris 06, CNRS UMR 7614, 11, rue P. et M. Curie, 75005 Paris, France

<sup>3</sup>INSP, UPMC Paris 06, CNRS UMR 7588, 140 rue de Lourmel, 75015 Paris France

<sup>4</sup>Sincrotrone Trieste S.C.p.A., Area Science Park, S.S.14, Km. 163.5, I-34012 Trieste, Italy

<sup>5</sup>Departamento de Física, Universidade Federal de Minas Gerais, CP 702, 30123-970 Minas Gerais, Brazil

<sup>6</sup>CNEA-Centro Atómico Bariloche and Instituto Balseiro-UNCuyo, R8402AGP San Carlos de Bariloche, Argentina  
(Received 20 November 2007; revised manuscript received 18 January 2008; published 10 April 2008)

We investigated the magnetic behavior of a 5 nm thick Fe layer deposited on a ferromagnetic MnAs/GaAs(001) template by using resonant magnetic scattering of polarized soft x rays. The Fe film displays in-plane uniaxial anisotropy and its magnetization can be modified and reversed by fine-tuning the substrate temperature around ambient because of the self-organization of the coexisting ferromagnetic and paramagnetic phases of the template.

DOI: [10.1103/PhysRevB.77.165317](https://doi.org/10.1103/PhysRevB.77.165317)

PACS number(s): 75.70.-i, 75.30.Gw, 73.21.Ac, 75.60.Jk

## I. INTRODUCTION

Self-organization is a promising approach to the growth of magnetic objects with controlled shape and magnetic anisotropies, which offers an alternative to lithography techniques. The prospect of developing rapid and cost effective processes motivates the investigation of magnetic structures with lateral dimensions ranging from micron size down to the atomic scale, which are grown by various bottom-up approaches such as step decoration of vicinal surfaces,<sup>1</sup> ion etching under grazing incidence,<sup>2</sup> or the growth on self-organized templates.<sup>3</sup>

In this paper, we present a study of the magnetic properties of a Fe film displaying a strong shape induced uniaxial anisotropy. The most important characteristic that we observe is that it is possible to reverse the Fe magnetization by simply changing the sample temperature by a few degrees around room temperature, which is either at remanence or under the action of a magnetic field. To obtain Fe with the desired morphology and magnetic properties, we prepared the samples on a magnetic self-organized template: MnAs thin films grown on GaAs(001) substrates.

MnAs/GaAs(001) films can display a regular array of troughs that are a few microns long, with a period of a few tens of nanometers (see Fig. 1). Scanning tunneling microscopy (STM) measurements show that these troughs are present at all temperatures between 100 and 400 K, forming the template for the growth of a Fe film with periodic corrugation. An additional feature of the MnAs/GaAs(001) substrate is the formation, at around room temperature, of ordered stripes originating from the self-organized coexistence of two structural phases. Bulk MnAs is in the ferromagnetic (FM)  $\alpha$  phase (hexagonal) up to about 40 °C, where it undergoes a first order phase transition to the paramagnetic  $\beta$  phase (orthorhombic).<sup>4</sup> MnAs films grown on GaAs display a more complex structural and magnetic transition, leading to an extended temperature region where  $\alpha$  and  $\beta$  phases coex-

ist. This phase coexistence has been experimentally observed in MnAs films grown on both (001) and (111) surfaces of the GaAs substrate.<sup>5,6</sup> In the case of MnAs/GaAs(001), ordered stripes alternating with the two phases are observed over a relatively wide temperature range ( $\sim 10\text{--}40$  °C).<sup>5</sup> The stripes form parallel to the  $c$  axis of MnAs ( $y$  direction in the inset of Fig. 1) and perpendicular to the easy magnetic axis of  $\alpha$ -MnAs. The temperature dependence of the morphology and that of the magnetic properties of the stripes are found to vary with the MnAs layer thickness over the range of

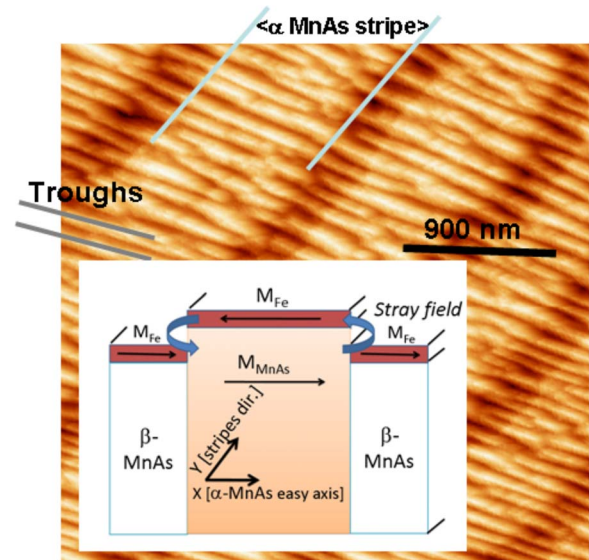


FIG. 1. (Color online) Room temperature STM image of the MnAs/GaAs(001) template before Fe deposition. Stripes form parallel to the  $c$  axis of MnAs ( $y$  direction in the figure), alternating with the  $\alpha$  (bright) and  $\beta$  (dark) phases. Shorter period troughs are visible normal to the stripes. Inset: schematic view of the sample geometry and of the stray-field induced magnetization reversal of Fe magnetization.

30–200 nm, with the thicker layers displaying larger periods of the stripes.<sup>7,8</sup>  $\alpha$ -phase and  $\beta$ -phase stripes have different heights, the step between them being of the order of 5% of the film thickness.<sup>8</sup>

The work presented in this paper stems from the idea that the interaction between such a complex material and a standard FM layer such as Fe can be tuned by the substrate temperature, acting, e.g., on lateral confinement and/or on magnetic coupling.<sup>9</sup> The technique we chose for this first investigation of the Fe/MnAs/GaAs(001) system is x-ray resonant magnetic scattering (XRMS) since it selectively gives a simultaneous description of both the structural and magnetic properties of the sample element.<sup>10</sup> Together with a large probing depth, element selectivity is an essential feature for separately analyzing the magnetic behaviors of MnAs and of Fe and to compare them.

## II. EXPERIMENTAL DETAILS

The sample was prepared by molecular beam epitaxy. After oxide desorption under As flux, a thick GaAs buffer layer was grown on the GaAs(001) substrate at 560 °C in As-rich conditions. The sample temperature was then reduced to 230 °C. The growth of the 130 nm thick MnAs film followed the procedure described by Tanaka *et al.*<sup>11</sup> to obtain a MnAs film with *A* orientation, as it was confirmed *in situ* by reflection high energy electron diffraction (RHEED) analysis and *ex situ* by x-ray diffraction. The 5 nm Fe layer was deposited by using a Knudsen cell on the MnAs substrate kept at a temperature of 160 °C, where MnAs is single phased ( $\gamma$  phase) and does not display any stripes.<sup>12</sup> *In situ* RHEED and *ex situ* transmission electron microscopy analyses showed that Fe epitaxially grows on MnAs, with  $(2-11)_{\text{Fe}} \parallel (1-100)_{\text{MnAs}} \parallel (001)_{\text{GaAs}}$  and  $[11-1]_{\text{Fe}} \parallel [001]_{\text{MnAs}} \parallel [1-10]_{\text{GaAs}}$ . Finally, the Fe layer was capped by 4 nm of ZnSe for protection during the transportation in air.

XRMS experiments were carried out at the circular polarization beamline<sup>13</sup> of the synchrotron ELETTRA (Trieste) by using the reflectometer IRMA (Ref. 14) and at the 6.3.2 beamline<sup>15</sup> of the synchrotron ALS (Berkeley). The circular polarization rates of the x rays were 70% and 50%, respectively. The energy resolving power was set to 2500 at both beamlines. For all the measurements, we used the same sample holder, which was fitted with a Peltier device for temperature control (–10 to 80 °C) and with an electromagnet (up to 1.5 kOe at the sample position). According to Fig. 1, *x* is the direction normal to the stripes, *y* is along the stripes, and *z* is the surface normal. In terms of exchanged momentum  $\mathbf{q}$ , specular reflectivity measurements correspond to  $q_z$  scans at  $q_x=q_y=0$ . We also performed rocking scans at constant  $q_z$  in coplanar geometry, with the stripes oriented either normal ( $q_x$  scans at  $q_y=0$ ) or parallel ( $q_y$  scans at  $q_x=0$ ) to the scattering plane.

## III. RESULTS

Figure 2 shows scattering data obtained with the stripes aligned parallel to the scattering plane. The photon energy

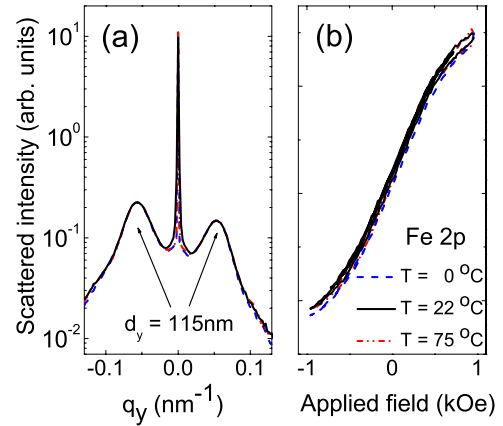


FIG. 2. (Color online) Scattered intensity ( $q_x=0$ ,  $\hbar\omega=707$  eV) at three temperatures corresponding to the  $\alpha$  phase ( $T=0$  °C)  $\beta$  phase ( $T=75$  °C), and phase coexistence ( $T=22$  °C) of MnAs: (a)  $q_y$  rocking scans; (b) specular reflectivity vs applied magnetic field.

was 707 eV (Fe 2*p* resonance) and data were collected at three temperatures:  $T=0$  °C (MnAs in the FM  $\alpha$  phase),  $T=75$  °C ( $\beta$  phase), and  $T=22$  °C (phase coexistence and stripe formation). Figure 2(a) shows the result of  $q_y$  scans at constant  $q_z=0.625$  nm<sup>–1</sup>. The two broad peaks centered at  $q_y=\pm 0.055$  nm<sup>–1</sup> correspond to an order parameter  $d_y=115$  nm that can be readily associated with Fe covering the troughs visible in Fig. 1. The same result was obtained by working at the Mn 2*p* resonance (640 eV) and also off resonance (600 eV). Apart from an increased diffuse scattering close to the specular ridge at  $T=22$  °C, all the three scans display identical features, indicating that the short period of the MnAs troughs and, consequently, of the Fe deposited on top of them, is not affected by the phase transformation nor by the formation and disappearance of stripes. Figure 2(b) shows field dependent specular reflectivity curves, which are sensitive to the magnetization of the Fe layer only. No remanence is observed at any temperature and the three curves, once normalized to the same total amplitude, look identical. We conclude that *y* is always a hard axis for the magnetization of the Fe film and that the troughs have the important role of defining a uniaxial anisotropy at every temperature, i.e., regardless of the MnAs magnetic properties and of stripe formation. This explains the persistence of in-plane easy and hard axes for the Fe layer even when the MnAs template is in its paramagnetic phase. By a simple magnetostatic model, we can estimate the anisotropy contribution associated with the troughs to be an order of magnitude larger than the bulk iron magnetocrystalline anisotropy, favoring the *x* direction as the easy magnetization axis. A strong temperature dependence is observed when the exchanged momentum is directed along *x*. Figure 3 shows a series of  $q_x$  rocking scans (at  $q_z=1.85$  nm<sup>–1</sup>) measured as a function of temperature with the *c* axis of MnAs oriented perpendicular to the *xz* scattering plane. As in Fig. 2, the photon energy is tuned to the Fe 2*p* resonance and the polarization is elliptical. When the temperature is lowered from 38 to 26 °C, we observe a strong reduction in the specular intensity and the formation of sharp peaks at  $|q_x|=0.0068$  nm<sup>–1</sup>, corresponding to a period of  $d_x=924$  nm, with maximum intensity at  $T=29$  °C.

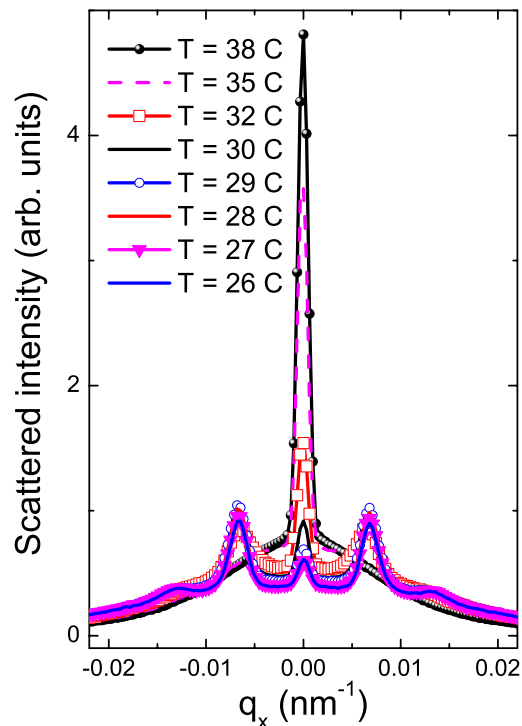


FIG. 3. (Color online)  $q_x$  rocking scans ( $q_y=0$ ,  $q_z=1.85 \text{ nm}^{-1}$ ) measured as a function of temperature upon cooling. Photon energy is 707 eV.

Second order peaks become visible at the lowest temperatures. This behavior is equivalent to what was already reported for MnAs/GaAs(001) layers alone<sup>16</sup> and it corresponds to the formation of the regular network of stripes alternating with the  $\alpha$  and  $\beta$  phases.

Figure 4(a) shows the temperature dependence of the specular reflectivity at the Fe 2*p* (squares) and Mn 2*p* (circles) resonances. The filled and open symbols correspond to increasing and decreasing temperatures, respectively. For each point, two measurements were performed at remanence after a magnetic pulse of 600 Oe, the field being either parallel or antiparallel to the photon helicity. The curves in the top panel are the average of the two measurements, representing the magnetization averaged specular reflectivity. The

temperature dependence at the Mn 2*p* and Fe 2*p* resonances is very similar: when the  $\alpha$  and  $\beta$  phases coexist between 13 and 40 °C, the reflectivity decreases because of the stripe formation, with a slight hysteresis (approximately 2 °C wide) on the low temperature side. Asymmetry ratio (AR) curves, defined as the difference divided by the sum of the two measurements performed after field pulses of opposite sign, are shown in the bottom panel of Fig. 4(a). The Mn magnetic signal steadily decreases with increasing temperature, with a sharp drop around 26 °C. The Fe magnetic signal shows a more complex behavior, with two changes in sign at 18.4 °C (16.5 °C upon cooling) and 29.5 °C. Therefore, an extended temperature region exists where the Fe layer and its MnAs template are coupled antiparallel. Mn and Fe have parallel magnetic moments at low temperature. When stripes set in, the Fe magnetic signal rapidly decreases, changes sign, then reaches a complete reversal at around 20 °C. When the Mn magnetic signal drops, the Fe layer begins a second magnetization reversal process that reaches completion around 40 °C, when the phase coexistence terminates and the stripes disappear. In order to better illustrate the magnetic coupling in the phase coexistence regime, in Fig. 4(b), we show the field dependent reflectivity measurements performed at a constant temperature of 22 °C. By tuning the photon energy at the Fe 2*p* (top) and Mn 2*p* (bottom) resonances, one obtains element selective hysteresis curves that correspond in our case to the average magnetization of the Fe layer and that of the MnAs template. MnAs has an almost square hysteresis loop with a coercive field of approximately 75 Oe, in very good agreement with previous results obtained on similar samples.<sup>16</sup> On the other hand, the Fe layer has a complex dependence of the magnetization on the applied field. Above 800 Oe, the Fe magnetization is aligned by the external field and it is parallel to the MnAs magnetization. At lower fields, Fe tends to couple antiparallel to the MnAs layer and its magnetization progressively reverses. In the low field region ( $\pm 250$  Oe), the antiparallel coupling is almost complete and the Fe magnetization switches sign exactly at the MnAs coercive field [thin dotted vertical lines in Fig. 4(b)].

Finally, Fig. 4(c) shows that Fe and MnAs display rather independent hysteresis loops, with very different values for the coercive and saturation fields at every temperature, suggesting a very weak interlayer coupling.

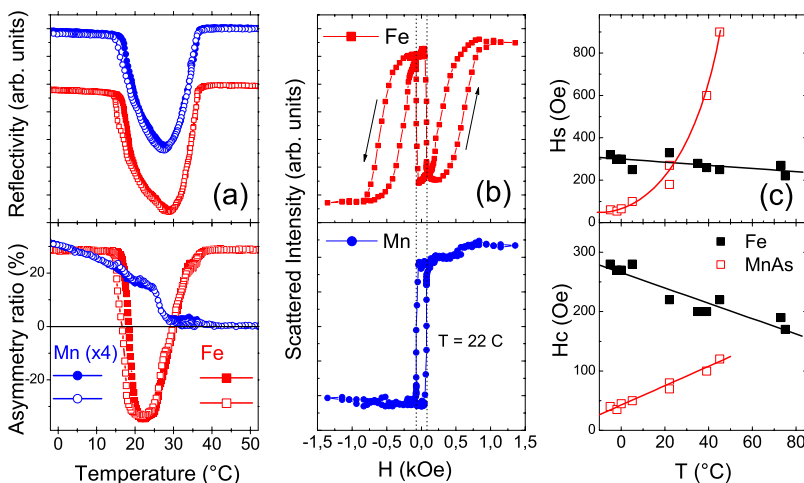


FIG. 4. (Color online) (a) Specular reflectivity vs temperature at  $\theta_S=15^\circ$  measured at remanence after a magnetic pulse of 600 Oe. Top: magnetization averaged reflectivity. Bottom: asymmetry ratio. The open and solid symbols refer to cooling down and warming up, respectively. (b) Specular reflectivity vs applied magnetic field at  $T=22^\circ\text{C}$ . Photon energies are 640 eV (bottom) and 707 eV (top). (c) The temperature dependent coercive field  $H_c$  (bottom) and saturation field  $H_s$  (top) values were derived from element selective hysteresis curves. The full and open symbols refer to Fe and MnAs, respectively. The lines are a guide to the eyes.

#### IV. DISCUSSION

Our X RMS investigation of the magnetic properties of an Fe layer deposited on MnAs/GaAs(001) allows us to point out that the relative orientation between the Fe and the MnAs magnetizations strongly varies with temperature. When both films are homogeneous and ferromagnetic (MnAs in the low temperature  $\alpha$  phase), the remanent magnetizations along the  $x$  axis are aligned parallel. By increasing the temperature, the formation of the stripes (and of the steps that go with them) modifies this situation, leading to the complex coupling shown in Fig. 4. The most striking variation in the Fe magnetization takes place over the temperature range of 15–20 °C, where MnAs is mostly in its  $\alpha$  phase, suggesting that the morphological modifications of the MnAs film rather than its magnetic transition drive the magnetization reversal of Fe.

This phenomenon can be ascribed to the dipolar interaction between the  $\alpha$ -MnAs stripes and the Fe overlayer, in the assumption of a very weak interlayer magnetic coupling. At about  $T=15$  °C, the MnAs film is organized in large  $\alpha$  domains separated by very narrow and long  $\beta$  regions in a sort of a raketlike groove pattern. The stray field due to the finite size of the  $\alpha$ -MnAs domains is superimposed on the external field  $H$  to determine the effective magnetic field  $H_{\text{eff}}$  that acts on Fe.  $H_{\text{eff}}$  will vary along the vertical direction within the Fe layer, but a simple way to estimate its maximum value is to apply Stokes' theorem to the Fe/MnAs interface. Since the directions of the applied magnetic field ( $H$ ) and that of the  $\alpha$ -MnAs magnetization ( $M$ ) are parallel to the interface and the Fe film is very thin,  $H_{\text{eff}}$  is equal to the inner field, i.e.,  $H-DM$ , where  $D$  is the demagnetizing factor. The demagnetizing factor of MnAs stripes can be estimated by applying the Aharoni formula<sup>17</sup> to a prism with dimensions of 700, >1000, and 130 nm along the  $x$ ,  $y$ , and  $z$  directions, respectively (these values refer to a MnAs  $\alpha$  stripe at 22 °C, see also Fig. 1). The resulting demagnetizing factor in the  $x$  direction is  $D\sim 2.2$  (cgs units). The MnAs magnetization at 22 °C is estimated to be about 330 emu/cm<sup>3</sup> based on a magnetization of  $\sim 650$  emu/cm<sup>3</sup> at 0 °C (Ref. 18) and on the experimental curve of Fig. 4(a), bottom panel. Finally, we obtain  $DM\approx 700$  Oe, which is a rough estimate of the maximum dipolar field generated by one  $\alpha$ -MnAs stripe and acting on the Fe layer deposited on top of it. Within the limits of our simple approach, this value agrees well with the shift of  $\sim 450$  Oe of the Fe loop that we experimentally observe [Fig. 4(b), top panel].

Neglecting the interlayer exchange is a drastic approximation that finds support in the temperature dependent data of

Fig. 4(c). In any case, our data indicate that exchange must be at least much smaller than the dipolar term estimated above. At the moment, we do not have a convincing explanation for the weakness of the interlayer magnetic coupling, although the formation of a thin ( $\sim 1$  nm) interdiffused interface layer may be at the origin of this effect. Compounds such as  $\text{Fe}_{a-x}\text{Mn}_x\text{As}$  ( $a$  close to 2,  $a > x > 0$ ) (Ref. 19) and FeMn (Ref. 20) are good candidates since they can present antiferromagnetic or ferrimagnetic characters.

By going back to Fig. 4(a) and considering increasing temperatures, the slopes of the first (starting at  $T=15$  °C) and second ( $T=23$  °C) magnetization reversals of Fe are quite different, the former being completed in less than 5°, while the latter extends over 15°. This can be explained by considering that, according to the model outlined above, the onset of the phase coexistence suffices to induce the appearance of a stray field and the reversal of the Fe magnetization. The second change in sign of the Fe magnetization, on the contrary, is driven by the continuous enlargement of the paramagnetic  $\beta$  stripes at the expense of the  $\alpha$  stripes. According to this picture, the Fe average magnetization should vanish when the  $\alpha$  and  $\beta$  stripes have equal width. This is confirmed by our scattering results, showing that at  $T=29-30$  °C, when the magnetic signal of Fe vanishes, the first order peak has a maximum (Fig. 3) and the specular reflectivity has a minimum [Fig. 4(a), top].

It is known that, as a function of temperature, an out-of-plane component of the MnAs magnetization can appear.<sup>16</sup> This may explain the sharp drop of the Mn signal at about 26 °C shown in Fig. 4(a) (bottom panel) and it has to be considered for a detailed analysis of the second magnetization reversal.

We have shown that the magnetization of Fe deposited on an MnAs film epitaxially grown on GaAs(001) can be modified and even reversed by changing the substrate temperature by a few degrees around room temperature. This phenomenon is due to the self-organization of the coexisting ferromagnetic and paramagnetic phases of MnAs in ordered stripes, the stray field of the  $\alpha$  phase favoring an antiparallel orientation of the Fe overlayer.

#### ACKNOWLEDGMENTS

We thank Dante Mosca (Universidad Federal do Parana, Curitiba, Brazil) and Coryn F. Hague for useful discussions and suggestions. The Agence Nationale de la Recherche (France) provided financial supports via the project MOMES. J.M. is a member of CONICET.

<sup>1</sup>A. Dallmeyer, C. Carbone, W. Eberhardt, C. Pampuch, O. Rader, W. Gudat, P. Gambardella, and K. Kern, Phys. Rev. B **61**, R5133 (2000).

<sup>2</sup>R. Moroni, D. Sekiba, F. Buatier de Mongeot, G. Gonella, C. Boragno, L. Mattera, and U. Valbusa, Phys. Rev. Lett. **91**, 167207 (2003).

<sup>3</sup>B. Borca, O. Fruchart, Ph. David, A. Rousseau, and C. Meyer, Appl. Phys. Lett. **90**, 142507 (2007).

<sup>4</sup>C. P. Bean and D. S. Rodbell, Phys. Rev. **126**, 104 (1962).

<sup>5</sup>V. M. Kaganer, B. Jenichen, F. Schippan, W. Braun, L. Däweritz, and K. H. Ploog, Phys. Rev. Lett. **85**, 341 (2000).

<sup>6</sup>N. Mattoso, M. Eddrief, J. Varalda, A. Ouerghi, D. Demaille, V.

- H. Etgens, and Y. Garreau, *Phys. Rev. B* **70**, 115324 (2004); V. Garcia, Y. Sidis, M. Marangolo, F. Vidal, M. Eddrief, P. Bourges, F. Maccherozzi, F. Ott, G. Panaccione, and V. H. Etgens, *Phys. Rev. Lett.* **99**, 117205 (2007).
- <sup>7</sup>L. Däweritz, L. Wan, B. Jenichen, C. Herrmann, J. Mohanty, A. Trampert, and K. H. Ploog, *J. Appl. Phys.* **96**, 5056 (2004).
- <sup>8</sup>M. Kästner, C. Herrmann, L. Däweritz, and K. H. Ploog, *J. Appl. Phys.* **92**, 5711 (2002).
- <sup>9</sup>During the review process of this paper, a paper was published [M. Zhu, M. J. Wilson, B. L. Sheu, P. Mitra, P. Schiffer, and N. Samarth, *Appl. Phys. Lett.* **91**, 192503 (2007)] reporting exchange-bias effects in the MnAs/(Ga,Mn)As FM-metal/FM-semiconductor interface.
- <sup>10</sup>C. Spezzani, M. Fabrizio, P. Candeloro, E. Di Fabrizio, G. Panaccione, and M. Sacchi, *Phys. Rev. B* **69**, 224412 (2004).
- <sup>11</sup>M. Tanaka, J. P. Harbison, and G. M. Rothberg, *J. Cryst. Growth* **150**, 1132 (1995).
- <sup>12</sup>R. H. Wilson and J. S. Kasper, *Acta Crystallogr.* **17**, 95 (1964).
- <sup>13</sup><http://www.elettra.trieste.it/experiments/beamlines/polar/index.html>
- <sup>14</sup>M. Sacchi, C. Spezzani, P. Torelli, A. Avila, R. Delaunay, and C. F. Hague, *Rev. Sci. Instrum.* **74**, 2791 (2003).
- <sup>15</sup><http://www-als.lbl.gov/als/techspecs/bl6.3.2.html>; J. H. Underwood, E. M. Gullikson, M. Koike, P. J. Batson, P. E. Denham, K. D. Franck, R. E. Tackaberry, and W. F. Steele, *Rev. Sci. Instrum.* **67**, 3372 (1996).
- <sup>16</sup>R. Magalhães-Paniago, L. N. Coelho, and B. R. A. Neves, *Appl. Phys. Lett.* **86**, 053112 (2005); L. N. Coelho, B. R. A. Neves, R. Magalhaes-Paniago, F. C. Vicentin, H. Westfahl, R. M. Fernandes, F. Iikawa, L. Däweritz, C. Spezzani, and M. Sacchi, *J. Appl. Phys.* **100**, 083906 (2006).
- <sup>17</sup>A. Aharoni, *J. Appl. Phys.* **83**, 3432 (1998).
- <sup>18</sup>L. Däweritz, *Rep. Prog. Phys.* **69**, 2581 (2006).
- <sup>19</sup>T. Kanomata, T. Goto, and H. Ido, *J. Phys. Soc. Jpn.* **43**, 1178 (1977).
- <sup>20</sup>F. Offi, W. Kuch, L. I. Chelaru, K. Fukumoto, M. Kotsugi, and J. Kirschner, *Phys. Rev. B* **67**, 094419 (2003).